J Mater Sci (2011) 46:1640–1645
DOI 10.1007/s10853-010-4980-8

Synthesis of manganese–zinc ferrite by powder mixing using ferric oxide from a steel mill acid recovery unit

S. S. Marins · T. Ogasawara · L. M. Tavares

Received: 19 November 2009 / Accepted: 4 October 2010 / Published online: 2 November 2010

Abstract With the aim of producing fine-grained manganese–zinc (Mn–Zn) ferrite at the end of a calcination process at moderate temperatures, this study consisted, at first, of an "electrochemically designed" powder mixing by wet-ball milling a mixture of manganese (MnO_2), zinc (ZnO), and iron (Fe_2O_3 granules produced by an acid recovery unit of a Brazilian steelmaker, milled to fine sizes using alkaline media) –based raw materials. This mixing/milling resulted in improved size reduction when compared to milling without any alkali addition. Further, noticeable size reduction was achieved when elemental Zn was used in place of ZnO, especially when ammonia was used as the medium. Calcination of the alkaline-milled mixture of $MnO_2 + ZnO + Fe_2O_3$ at 1200 °C allowed obtaining well-crystallized single-phase Mn–Zn ferrite, whereas calcination of the $MnO_2 + ZnO + Fe_2O_3$ mill-mixed in 100% NH_4OH at 1200 °C produced the highest saturation magnetization in the as-calcined state.

Introduction

The use of industrial byproducts in the production of high added value ceramics is beneficial from both economical and environmental viewpoints. In the case of ferrites, iron is the metal that represents the largest fraction in weight, so that searching for appropriate iron-bearing byproducts in industry is of great relevance. A rich iron-bearing material is generated as a byproduct of hydrochloric regeneration plants from pickling units of steel in several steel mills [1, 2]. These units are often based on spray-roasting, which is responsible for producing a material predominantly composed of ferric oxide in the form of millimeter-sized granules.

Manganese–zinc (Mn–Zn) ferrites are materials of great current interest, in particular due to their widespread application in electronics. Among their uses, Mn–Zn ferrites are applied as magnetic refrigerant, replacing vapor-phase refrigeration [3], and as core materials for transformers [4]. Doping has been recognized as an important tool to alter significantly the properties of the Mn–Zn ferrite [5–7]. For instance, it has been demonstrated that the power loss and initial permeability fluctuate with increasing MoO_3 content, and magnetic properties can be improved with suitable additions of MoO_3, such that 400 ppm of TiO_2 provided 5.78% reduction in the power loss [8]. Power loss can also be reduced by Sn^{4+} additions, which is additionally responsible for an increase in initial permeability [4]. It has also been found that the grain size and density of Mn–Zn ferrites decrease while electrical resistivity increases with increased additions of NiO [9]. Microstructure-modifying liquid phase forming additives (e.g., SiO_2) were found to influence directly the final density of the Mn–Zn ferrite ceramics [5]. Finally, research found that by an appropriate control of processing variables, it was possible to enhance the specific grain-boundary resistivity, which led to higher frequency stability of the magnetic permeability [10].

Synthesis of this class of ceramics also remains attracting the attention of researchers, which is evident from the several publications on the subject in recent years.

T. Ogasawara is deceased.

S. S. Marins
Petrobrás, Rio de Janeiro, RJ, Brazil

T. Ogasawara · L. M. Tavares (✉)
Department of Metallurgical and Materials Engineering,
Universidade Federal do Rio de Janeiro—COPPE/UFRJ,
Cx. Postal 68505, CEP 21941-972, Rio de Janeiro, RJ, Brazil
e-mail: tavares@metalmat.ufrj.br

Examples are investigations associated to the development of new methods for synthesis [11–14], improvement of metal–organic precursor methods [15], development of nanotechnologies [16, 17], and improvement in the powder forming and sintering processes [18–22].

This article is concerned with the synthesis and characterization of Mn–Zn ferrite through an innovative powder mixing method in which a mixture of starting raw powder materials, including spray-roasted ferric oxide granules generated as a byproduct of a hydrochloric acid regeneration unit of a major Brazilian steel mill, was used. The innovative feature of the method consisted of performing the powder mixing through electrochemically assisted ball milling [23], which aimed at reducing the synthesis temperature and thereby reducing crystal size of the Mn–Zn ferrite in the calcined product. It is hoped that the synergic use of increased pH and the reduced potential during electrochemically assisted ball milling will allow enhanced reduction in particle sizes during milling, dissolution of iron oxide into the aqueous medium, resulting in the removal of the kinetics barrier in the formation of the ferrites. When coupled to a hydrolysis conducted after milling, through which the pH was reduced and the oxygen potential increased, conditions would be suitable for the formation of very fine oxide/hydroxide precipitated within the aqueous medium. The very fine iron oxide feedstock generated using this method is hoped to be better suited for more intimate powder mixing, thereby allowing ceramic synthesis under lower calcination temperature, also leading to a more limited trend toward agglomeration of the ceramic powders.

Experimental

Ferric oxide granules generated by spray-roasting in a hydrochloric acid recovery unit of a major Brazilian steel mill were used as the feedstock of Fe_2O_3. Their composition (wt%) was determined by X-ray fluorescence as 99.22% Fe_2O_3 and 0.78% SiO_2. Analytical grade chemicals have been used as feedstocks for NaOH, NH_4OH, MnO_2, $MnCO_3$, Zn, and ZnO. The ferric oxide granules (having particle sizes: 99.4 wt% $<$ 2,200 μm, 24.0 wt% $<$ 1,000 μm, 4.5 wt% $<$ 500 μm, and 0.4 wt% $<$ 250 μm, determined by sieving) were pre-ground in dry mode in a cylindrical steel grinding mill (180 mm diameter, 230 mm length, with 5 L capacity) with 20-mm diameter steel rods as grinding media, 20% volume filling with grinding media, 40% filling of void space, 68 rpm of mill rotating speed) for 1 h to crush the initial tough granules. The particle size distribution of this pre-milled ferric oxide is given by 99.6 wt% $<$ 1.410 μm, 95.4 wt% $<$ 1.000 μm, 83.7 wt% $<$ 710 μm, 59.0 wt% $<$ 425 μm, 33.5 wt% $<$ 210 μm, 11.6 wt% $<$ 106 μm.

The powder mixture was milled in the same cylindrical mill used in the pre-grinding experiments but using steel balls measuring 20 mm of diameter as grinding media. The experiments were conducted in wet mode, in aqueous solutions of NaOH (1 or 0.5 M) or NH_4OH (100 or 50 vol%) forming a slurry containing 7 wt% of solids for 5 h of milling. After milling, the solid/liquid separation was performed by repeating twice the procedure of dilution using distilled water, letting the solids settle, siphoning, before drying. The particle size distribution of the resulting powder was measured by laser diffraction and the specific surface area by BET.

Table 1 presents the compositions for all the test conditions used in chemically assisted milling: two of them (containing ZnO addition) resulted actually in electrochemically assisted milling, since reductive oxygen potential was achieved during milling.

Samples produced by these chemically controlled ball milling-mixing tests for each of the mixtures listed in Table 1 have been calcined for 4 h in air at 1200 °C and then cooled inside the same muffle furnace. X-ray diffraction analyzes were carried out for each sample to determine the phases present in the final calcination product, while analyzes by scanning electron microscopy have been conducted to illustrate the corresponding particle morphologies. Additionally, samples of the calcined products were submitted to measurements using a Vibrating Sample Magnetometer to characterize the magnetic properties.

Results and discussion

Table 1 shows a summary of the results of the chemically (and electrochemically) assisted grinding experiments. It demonstrates that the materials with the highest specific surface areas were obtained from grinding using ammonia (test-mixtures 4 and 7) while the finest representative particle sizes were reached using electrochemically assisted milling (test-mixtures 6 and 7). Indeed, a comparison of results from test-mixtures 3 and 6, as well as 4 and 7, demonstrates the role of electrochemically assisted milling in increasing the specific surface area through the reduction of particle sizes.

Chemically assisted milling was also found to be capable of reducing particle sizes, and evidence is demonstrated from a comparison of results from experiments using the test-mixtures 1–5. It was also found that surface area decreased when using NaOH (presumably due to preferential removal of surface roughness), while it increased when ammonia was used. Additional explanations on these differences may be associated to the fact that the solution pH value is higher whenever 1 M NaOH was used in milling in comparison to 100% NH_4OH, although

Table 1 Particle size distribution and BET surface area of the milled-mixed powder mixtures and magnetic properties after calcinations at 1200 °C

Test-mixture		D_{90} (μm)	Surface area (m^2/g)	M_s		H_s (kOe)	H_c (kOe)	M_r (emu/g)	μ_i (emu/g) × 100[b]
No.	Composition[a]			emu/g	G				
1	MnO_2 + ZnO	8.45	9.7	32.7	4109	4.45	0.29	19.8	1.034
2	MnO_2 + ZnO 1 M NaOH	6.63	6.7	38.9	4888	5.63	0.30	25.7	8.833
3	MnO_2 + ZnO 0.5 M NaOH	6.60	7.8	37.0	4849	4.30	0.25	20.8	5.393
4	MnO_2 + ZnO 100% NH_4OH	5.16	10.6	35.0	4398	5.75	0.28	21.5	5.943
5	$MnCO_3$ + ZnO 1 M NaOH	5.14	7.2	35.7	4486	6.36	0.32	23.2	3.718
6	MnO_2 + ZnO 0.5 M NaOH	3.74	10.1	34.6	4348	5.18	0.33	21.7	4.237
7	MnO_2 + ZnO 100% NH_4OH	3.80	14.4	40.1	5039	1.26	0.24	25.6	6.983

[a] All compositions contain additionally Fe_2O_3

[b] For H = 1 Oe

ammonia has the added capability of depressing oxygen potential in aqueous solution (readily demonstrated in a Pourbaix diagram [24] of electrochemical potential vs. pH for the nitrogen–water system, NH_4^+(aq)/HNO_3(aq) and NH_4OH(aq)/NO_3^-(aq) equilibria) while NaOH does not undergo any oxidation/reduction equilibrium in the standard stability domain of liquid water. Further explanations for this difference may be found elsewhere [23].

Figure 1 presents the XRD patterns of the seven test-mixtures after calcination at 1200 °C for 4 h in air. It is evident that almost all of the test-mixtures achieved complete formation of the single-phase Mn–Zn ferrite (hollow squares), with only the control–test mixture 1 presenting traces of hematite (dark-filled square) and test-mixture 4 showing traces of $ZnFe_2O_4$ (dark-filled lozenge) and eventual traces of Fe_3O_4 might be evaluated by Rietveld refinement. On the other hand, calcinations at 1200 °C for 4 h were sufficient to achieve single-phase Mn–Zn ferrite. Indeed, it is likely that lower temperatures could be used to produce the desired single-phase Mn–Zn ferrite from the different test-mixtures that were electrochemically milled, although such limiting temperatures were not investigated at this time.

Figure 2 shows scanning electron micrographs of all the 7 test-mixtures in their as-calcined stages at 1200 °C for 4 h in air. The control–test mixture 1 (Fig. 2a), as well as the test-mixtures 2 (Fig. 2b), 3 (Fig. 2c), and 7 (Fig. 2g) present angular spinel crystals with sizes in the range from about 1 to 5 μm, while test-mixtures 4 (Fig. 2d), 5 (Fig. 2e), and 6 (Fig. 2f) present finer grain-sizes (in average 2.5 μm in Figs. 2d and e and 1–2 μm in Fig. 2f). Therefore, no apparent relationship was identified between particle sizes of the powder before calcination and sizes of the grains resulting from calcination. This is not surprising, since the reaction between the starting components (manganese oxide, zinc metal or oxide, and iron oxide) generates Mn–Zn crystals whose sizes increase continuously, with the coarser particles growing at the expense of finer particles and the remaining amorphous reactants.

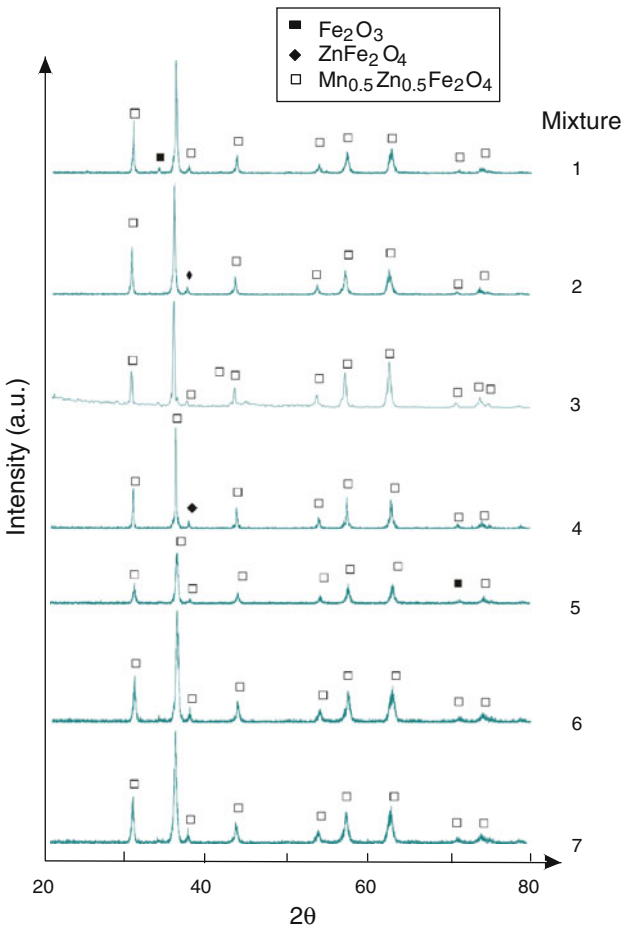

Fig. 1 XRD patterns of the test-mixtures after calcinations at 1200 °C for 4 h in air

Figure 3 presents magnetic hysteresis curves as determined by Vibrating Sample Magnetometer on samples of

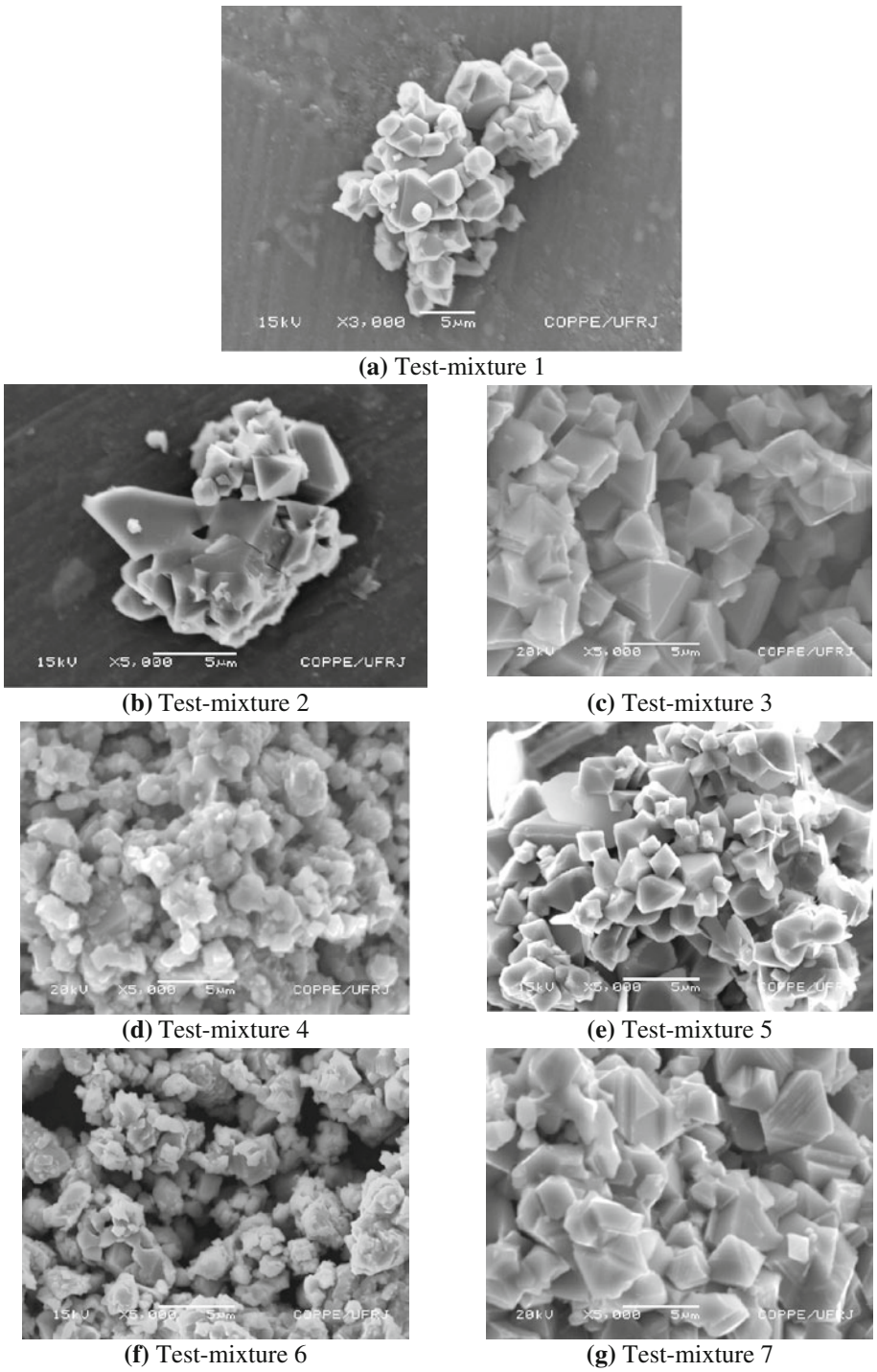

Fig. 2 Scanning electron micrographs of the calcined product

(a) Test-mixture 1

(b) Test-mixture 2

(c) Test-mixture 3

(d) Test-mixture 4

(e) Test-mixture 5

(f) Test-mixture 6

(g) Test-mixture 7

calcined Mn–Zn ferrite powders. Data from Fig. 3 and Table 1 show that saturation magnetization (M_s) is highest for test-mixture 7 (Fig. 3b), followed by the values obtained for test-mixtures 2 and 3, with the lowest value corresponding to test-mixture 1 (Fig. 3a). The same ranking of the results was found for initial permeability (μ_i), as showed in Table 1.

The optimal values of saturation magnetization (M_s) obtained in this study are in the order of 38–40 emu/g, achieved with magnetic field intensities below 10 kOe (Table 1). These values are well above 26 emu/g, which was the one obtained by Maiorov et al. [25] with Mn–Zn ferrite, $Mn_{0.5}Zn_{0.5}Fe_2O_4$, indicating that good quality spinel ferrites have been obtained in this study. Further, in this study a saturation magnetization higher than the value (0.84 kG or 0.56 emu/g) found by Skolyszewska et al. [35] with $(Mn_{0.56}Zn_{0.35}Fe_{0.1})Fe_2O_4$ was obtained. The Mn–Zn ferrite produced by these researchers [35] using the

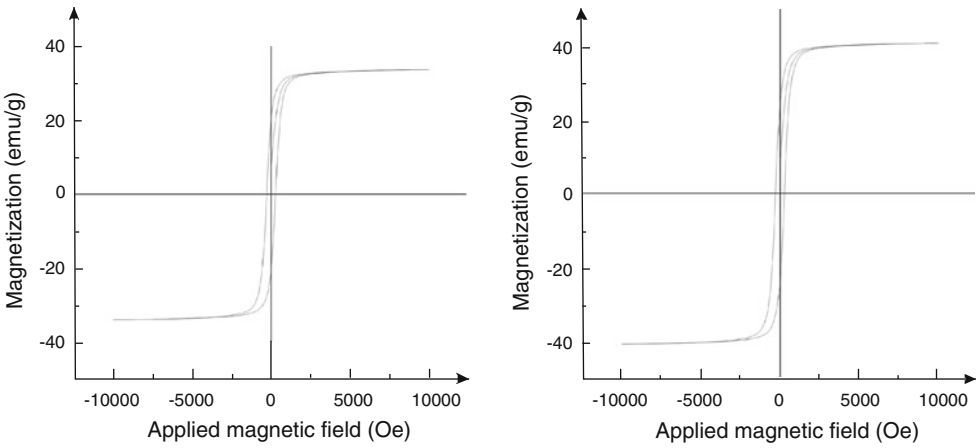

Fig. 3 Magnetic hysteresis curves of selected calcined test-mixtures, as determined by Vibrating Sample Magnetometer: test-mixture 1 (*left*) and 7 (*right*)

conventional ceramic powder mixing method, with calcinations in at a temperature in the range from 900 to 1050 °C during 1.5 h.

Rozmann and Drofenik [26] pointed out that the formation of spinel Mn–Zn ferrite is associated to the presence of Mn^{2+} and depends strongly on the partial pressure of oxygen in the sintering atmosphere. This subject has been of major concern for many researchers working with Mn–Zn ferrites [27–35] and has been already analyzed by the authors in a previous publication [36]. In air, single-phase Mn–Zn ferrite might be formed above 900 °C, so that future experiments should be carried out with the starting raw materials of this study at different temperatures in the range from 900 to 1200 °C to evaluate the results aiming to achieve the optimal calcinations temperatures for each of the test-mixtures studied.

Conclusions

The investigation on the use of pre-ground ferric oxide granules from spray-roasting and hydrochloric acid recovery unit of a major Brazilian steel mill to produce Mn–Zn ferrite allowed to conclude that:

- ammonia-assisted milling was capable of producing noticeable increase in the surface area of the milled product
- alkaline milling of the ferric oxides mixed with elemental Zn (resulting in electrochemically assisted milling) was capable of significant particle size reduction of the milled product, which resulted in higher specific surface are whenever NaOH was used as the alkaline agent
- calcination at 1200 °C of the alkaline-milled mixture of $MnO_2 + ZnO + Fe_2O_3$ allowed to achieve well-crystallized single-phase Mn–Zn ferrite
- calcination at 1200 °C of the $MnO_2 + ZnO + Fe_2O_3$ mill-mixed in 100% NH_4OH produced the highest saturation magnetization of the powder after calcination.

Acknowledgements The authors are grateful to CNPq, CAPES and FINEP/PADCT for the financial support to this investigation.

References

1. Negro C, Latorre R, Dfour J, Formoso A, Mateos FL (1994) J Environ Sci Health A 29(2):1899
2. Beck M, Wirtz S, Scherer V, Barthold F (2007) Chem Eng Technol 30(10):1347
3. Mamiya H, Terada N, Furubayashi T (2010) J Magn Magn Mater 322(9–12):1561
4. Ji HN, Lan ZW, Yu Z (2009) J Magn Magn Mater 321(14):2121
5. Shokrollahi H, Janghorban K (2007) Mater Sci Eng B 141:91
6. Shokrollahi H (2008) J Magn Magn Mater 320:463
7. Liang TJ, Nien HH, Chen JF (2007) IEEE Transac Magn 43(10):3816
8. Gu M, Liu GQ (2009) J Alloys Comp 475(1–2):356
9. Sun K, Lan ZW, Yu Z (2009) Mater Chem Phys 113(2–3):797
10. Hanuszkiewicz J, Holz D, Eleftheriou E (2008) J Appl Phys 103(10):103907-1–103907-9
11. Kosak A, Makovec D, Drofenik M, Znidarsic A (2004) J Magn Magn Mater 272–276:1542
12. Makovec D, Kosak A, Znidarsic A, Drofenik M (2005) J Magn Magn Mater 289:32
13. Wang J, Chong PF, Ng SC, Gan LM (1997) Mater Lett 30:217
14. Yener DO, Giesche H (2001) J Am Ceram Soc 84(9):1987
15. Verma A, Chatterjee R (2006) J Magn Magn Mater 306(2):313
16. Poddar P, Srikanth H, Morrison SA, Carpenter EE (2005) J Magn Magn Mater 288:443
17. Arulmurugan R, Vaidyanathan G, Sendhilnathan S, Jeyadevan B (2006) J Magn Magn Mater 298:83
18. Skolyszewska B, Tokarz W, Przybylski K, Kakol Z (2003) Physica C 387:290
19. Arshak KI, Ajina A, Egan D (2001) Microelectron J 32:113
20. Mandanas MM, Shaffer W, Adair JH (2002) J Am Ceram Soc 85(9):2156
21. Mauczok R, Zaspalis VT (2000) J Eur Ceram Soc 20:2121
22. Suh JJ, Han YH (2003) J Am Ceram Soc 86(5):765
23. Marins SS (2006) Manganese–zinc ferrite synthesis by chemically aided milling and calcination. Ph.D. thesis, Department of Metallurgical and Materials Engineering, Universidade Federal do Rio de Janeiro, Brazil, p 154 (in Portuguese)

24. Pourbaix M (1974), Atlas of Electrochemical Equilibria in Aqueous Solutions, NACE, USA and CEBELCOR, Brussels (Belgium)
25. Maiorov M, Blums E, Hanson M, Johanson C (1999) J Magn Magn Mater 200:95
26. Rozman M, Drovenik M (1998) J Am Ceram Soc 81(7):1757
27. Janghorban K, Shokrollah H (2007) J Magn Magn Mater 308:238
28. Lezhong L, Zhongwen L, Zhong Y, Ke S, Haining J (2007) J Magn Magn Mater 318:39
29. Yapi L, Shijin H (2008) J Magn Magn Mater 320:3318
30. Ke S, Zhongwen L, Zhong Y, Lezhong L, Xiaoliang N, Zhiyong X (2009) J Alloys Comp 468:315
31. Haining J, Zhongwen L, Zhong Y, Ke S, Lezhong L (2009) J Magn Magn Mater 321:2121
32. Ateia E, Ahmed MA, El-Aziz AK (2007) J Magn Magn Mater 311:545
33. Morineau R, Paulus M (1975) IEEE Transac Magn 11:1312
34. Otobe S, Yachi Y, Hashimoto T, Tanimori T, Shigenagi T, Takei H, Hontani K (1999) IEEE Transac Magn 35(5):3409
35. Ming G, Gongqiang L (2009) J Alloys Comp 475:356
36. Ogasawara T, Tavares LM, Marins SS (2007) Mater Lett 61:5063